Stepwise Photoreactions and Photosalient Effects in Isostructural Donor-Acceptor Molecular Complexes with Tunable Optical Properties

Aditya Choudhury,† Narayan Prasad,‖,# Tejendra Banana,†,# Pyarija S. Lal,† David S. Hughes,§ Nathan R. Halcovitch,$ Md Mehboob Alam,*,†,‡ Sesha Vempati,*,‖ and Raghavender Medishetty,*,†,‡

† A. Choudhury, T. Banana, Dr. M. M Alam, Dr. R. Medishetty

Department of Chemistry, Indian Institute of Technology Bhilai, Durg, Chhattisgarh 491002, India. E-mail: mehboob@iitbhilai.ac.in, raghavender@iitbhilai.ac.in

‡ Dr. M. M Alam, Dr. R. Medishetty

Department of Materials Science and Metallurgical Engineering, Indian Institute of Technology Bhilai, Durg, Chhattisgarh 491002, India.

‖ N. Prasad, Dr. S. Vempati

Department of Physics, Indian Institute of Technology Bhilai, Durg, Chhattisgarh 491002, India. Email: sesha@iitbhilai.ac.in

$ Dr. N. R. Halcovitch

Chemistry Department, Lancaster University, Faraday Building, Lancaster University, Lancaster, LA1 4YB, UK.

§ Dr. D. S. Hughes

School of Chemistry, Faculty of Engineering and Physical Sciences, University of Southampton, Southampton SO17 1BJ, U.K.

# These are authors contributed equally.

KEYWORDS: Stepwise photoreaction, Donor-Acceptor, Isostructurality, Photosalient effect, Raman spectroscopy.

ABSTRACT: In the rapidly evolving field of molecular design, donor–acceptor complexes have garnered significant attention due to their unique optical, electronic, and photoreactive properties. This study explores the synthesis of donor–acceptor molecular complexes using electron-deficient tetrafluoroterephthalate and four electron-rich 4-vinylpyridine derivatives. Due to the similar chemical structures of 4-vinylpyridine derivatives (2tpy, 3tpy, 4spy, and 3F-4spy), three of the four complexes exhibit isostructural packing. These compounds display segregated arrangements and undergo [2+2] solid-state photoreactions even under ambient light, with stepwise structural evolution captured by single-crystal-to-single-crystal (SCSC) X-ray diffraction. Under UV irradiation, the crystals show single-step photoreactions along with distinct photosalient behavior. The charge-transfer nature of these complexes, which drives their photoreactivity under ambient light, is investigated through optical absorption studies and Raman spectroscopy. The vibrational signatures obtained from Raman experiments are further interpreted using TD-DFT calculations, offering detailed insight into the electronic structure and molecular interactions.

Locomotion is a fundamental aspect of nature, playing a crucial role in the evolution of life by enabling survival, reproduction, and various daily activities.[1] From the origin of life on

Earth to the present, movement has been essential for adaptation and progress. In addition to locomotion, sensory behavior is equally vital, allowing organisms to respond to environmental stimuli through mechanisms such as electrical impulses and pH changes. Inspired by these biological processes, scientists have developed various sensors that respond to external stimuli, including electrical signals, heat, and light.[2-5] Among these, light-driven sensors hold distinct advantages due to their remote activation, tunability across different wavelengths, precise intensity control, and ability to propagate in vacuum.[6] Mimicking natural mechanical motions, researchers have recently focused on designing next-generation sensors triggered by photochemical reactions.[7-15] In this regard, solid-state [2+2] photoreactions are considered one of the most effective methods for converting light energy into mechanical force.[16-22] This reaction offers significant advantages, such as the use of simple, easily synthesizable molecules and the ability to characterize photoreactions and photomechanical mechanisms with minimal ambiguity due to its often irreversible nature of the reaction.[23-27]

Stepwise photoreactions, where molecular units react sequentially, offer greater control over solid-state transformations, preserving material integrity while enabling precise modulation of structural and mechanical properties.[28] Unlike single-step reactions, they allow for capturing intermediate states, monitoring molecular rearrangements, and tailoring reaction kinetics—insights that are often lost in studies focusing solely on the initial and final stages of a reaction. In solid-state [2+2] photoreactions, slowing down the process and studying intermediates via X-ray diffraction provides crucial information about a deeper understanding of the influence of olefin separation distances, and configurational changes during the photoreaction.[29-34] Furthermore, this approach enables a deeper understanding of the influence of molecular rearrangements during the photoreaction, the reaction mechanism, and structural evolution

from monomer to dimer, paving the way for the design of programmable photoresponsive materials with enhanced functionality.[35-37]

Donor-acceptor (D-A) molecular complexes exhibit intriguing optical and electronic properties due to their distinctive band structure and other key characteristics. In recent years, D-A molecular systems have emerged as a promising avenue for various novel applications, including band gap tunability, enhanced conductivity, and optoelectronic functionalities.[38-39] The charge transfer ability and overall electronic behavior of these complexes are highly dependent on the molecular polarizability, which in turn is influenced by structural factors, substituents, and molecular packing. Traditionally, charge-transfer complexes have been studied using optical and computational methods, often in combination.[40] While vibrational spectroscopy, particularly Raman spectroscopy, is highly sensitive to changes in electron density, its use in directly confirming ground state charge-transfer behavior remains relatively unexplored. The systematic shifts in vibrational bands observed in Raman spectra provide valuable insights into electronic cloud distribution, making it a powerful yet underutilized tool for investigating charge-transfer interactions in molecular complexes.[41-45]

In this study, we successfully obtained four donor-acceptor molecular complexes by pairing electron-rich derivatives of 4-vinylpyridine (2tpy, 3tpy, 4spy, and 3F-4spy) with a common electron-withdrawing tetrafluoroterephthalate (TFT). The protonation of pyridine groups facilitated a head-to-tail alignment of the olefin moieties, enabling a solid-state [2+2] cycloaddition reaction while also exhibiting photosalient behavior. Although crystals exposed to UV light exhibit rapid photoreaction accompanied by photosalient effects, the mechanical strain causes the crystals to fracture and lose their integrity, making them unsuitable for X-ray data collection. By reducing the reaction rate under ambient sunlight, we successfully captured intermediate structures via single-crystal-to-single-crystal (SCSC) transformation. Meanwhile, the presence of a through space charge-transfer band in these complexes allowed for systematic

tuning of the optical properties by varying the donor molecule. Notably, the exchange of phenyl and thiophene units enabled the formation of isostructural complexes with minimal disruption to the solid-state packing, while inducing a controlled variation in the optical band gap based on the donor strength. Remarkably, the photoreaction proceeded even under ambient light conditions, attributed to the charge-transfer absorption bands, which were absent in the precursor molecules. These absorption bands not only expanded the photoreactivity spectrum but also enhanced reactivity. The charge-transfer mechanism was further validated through Raman spectroscopy and computational studies.

Pale yellow single crystals of $[(TFT)_2(H\text{-}2tpy)_4]$ (**1**) (where 2tpy = 4-(2-(thiophene-2-yl)vinyl)pyridine) were obtained via slow evaporation of a DMF solution containing TFT and 2tpy in a 1:2 molar ratio. The molecular complex crystallized in the triclinic *P*-1 space group (Z = 2), with the asymmetric unit comprising one TFT molecule and two protonated 2tpy linkers, forming a single molecular formula unit. The structure is stabilized by hydrogen bonding between the protonated pyridyl groups of 2tpy and the carboxylate moieties of TFT, creating a robust H-bonded hetero-synthon (Figure 1a and 1b). These interactions lead to a segregated stacking arrangement, where 2tpy molecules form columnar head-to-tail (HT) stacks, while TFT molecules pack separately (Figure 1c). With reference to the computation, the optimized ground state geometry of all the four systems is compared with their respective XRD data. We observed a very good agreement between the experimental and computational structures.

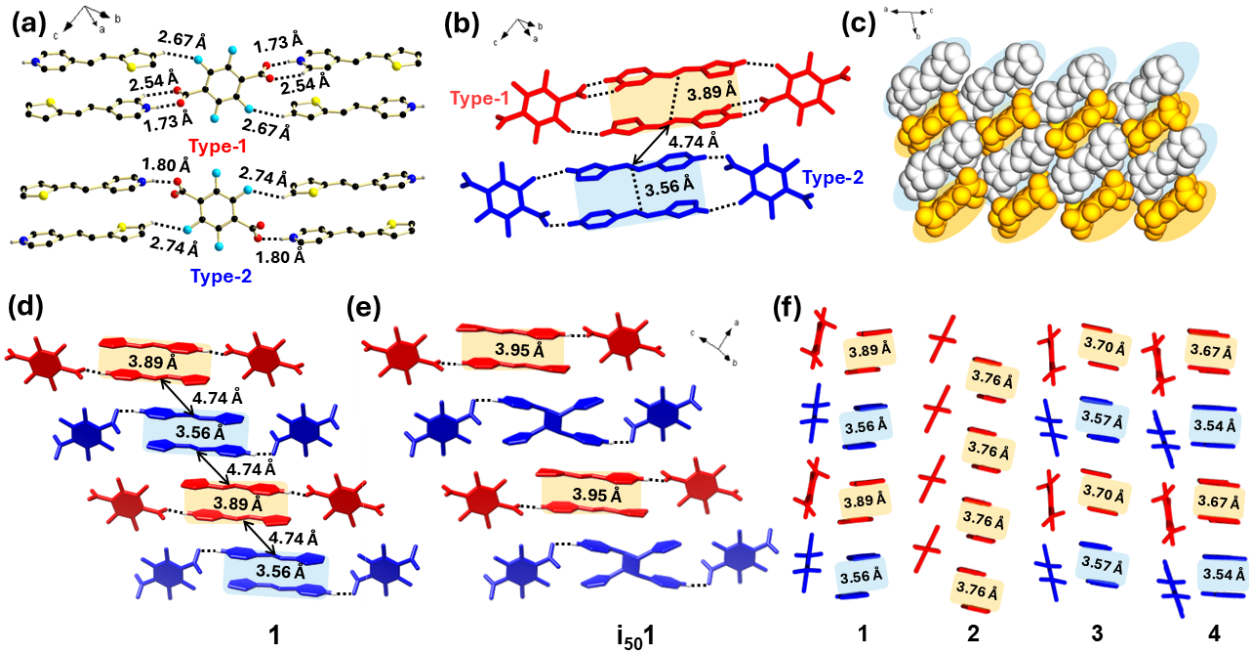

Figure 1. (a) Crystal structure of **1**, highlighting key hydrogen bonds and two distinct types of TFT molecules based on their interactions with 2tpy. (b) Packing arrangement showing two configurations of TFT–H-2tpy interactions and the corresponding olefinic separations between 2tpy linkers. (c) Space-filled model of **1**, illustrating the segregated packing of TFT and 2tpy. (d) Schematic view of the hydrogen-bonded TFT–2tpy assembly, indicating the alignment and distances between olefin groups. (e) Structure of intermediate $\mathbf{i_{50}1}$ after 50% photoreaction, highlighting changes in olefinic separations post-[2+2] cycloaddition. (f) Depiction of TFT molecules and 4-vinylpyridine derivatives in **1**–**4**, showing olefinic separations in each complex.

Strong interactions between the electron-rich thiophene and electron-deficient protonated pyridine moieties facilitate the precise alignment of olefin groups, resulting in distinct paired arrangements. Structural analysis revealed two types of olefinic separations: 3.56 Å in one pair and 3.89 Å in the other, both within Schmidt's criteria for photoreactivity (Figure 1b).[46] These aligned systems arise due to the presence of two different TFT-2tpy interactions, classified as Type-1 (**T1**) and Type-2 (**T2**) configurations. In the **T1** configuration, the pyridyl side of the

2tpy linkers interacts with the carboxylate group of TFT, forming a robust pyridyl-carboxylate H-bonded synthon in a characteristic $R_2^2(7)$ motif (Figure 1a). Meanwhile, in the **T2** arrangement, the protonated pyridyl group strongly interacts with one of the carboxylate oxygens of TFT. The coexistence of these two structural motifs suggests the potential for a stepwise photoreaction with quantitative yield.

As expected, ambient light irradiation induced a stepwise photoreaction in **1**. SCSC X-ray diffraction studies confirmed that the olefinic pair separated by 3.56 Å 2tpy linker (**T2** configuration) underwent complete photodimerization, while another pair at 3.89 Å which are present in **T1** configuration remained unreacted. This selective reaction resulted in a 50% conversion, forming an intermediate structure (**i$_{50}$1**; $[(TFT)_2(H\text{-}2tpy)_2(H_2\text{-}2ptcb)]$, where 2ptcb = *regio-cis, trans, trans*-1,3-bis(4'-pyridyl)-2,4-bis(2-thiophenyl)cyclobutane), which was stabilized within the crystal lattice (Figure 1e). The asymmetric unit of **i$_{50}$1** contains half of the **T2** TFT molecular unit with one complete **T2** H-2tpy molecule and half **T1** TFT molecular unit with half of the H_2-2ptcb molecule and the unit cell composed of two formula units, while the separation distance of unreacted 2tpy linkers has slightly increased to 3.95 Å.

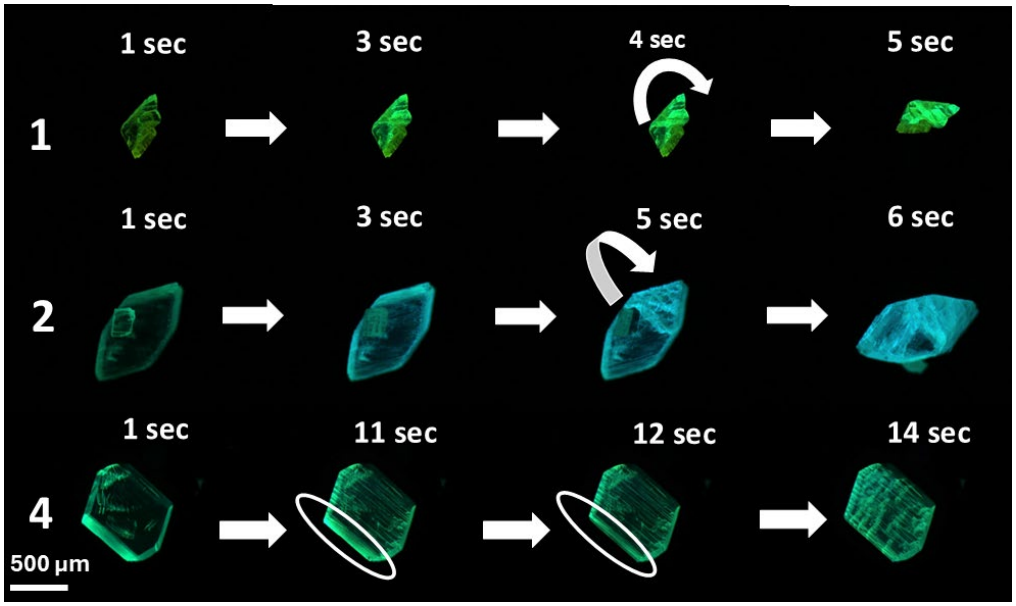

Figure 2. Photosalient behavior of **1**, **2** and **4** under UV light. **1** have shown rotation of the crystals while **2** exhibit flipping motion and in **4**, a part of the crystal jumped out rapidly under UV irradiation.

^{1}H NMR analysis confirmed quantitative photodimerization under both ambient and UV light. Unfortunately, further photoreaction leading to 100% conversion was not achievable under SCSC conditions as the single crystal did not survive. Time-dependent studies revealed that the photoreaction under UV light followed first-order like kinetics, with a rate constant of 7.7 x 10^{-3} min^{-1}, while ambient light irradiation proceeded slowly, exhibiting a break in the time-dimerization plot indicative of a stepwise process (See Figure S30-S45 and Table S3).

To investigate the effect of substitution position on the thiophene moiety without significantly altering structural features, 4-(3-(thiophene-3-yl)vinyl)pyridine (3tpy) was used as a substitute for 2tpy. Pale yellow single crystals of $[(TFT)_2(H\text{-}3tpy)_4]$ (**2**) were obtained using a procedure similar to that for **1**, crystallizing in the *P*-1 space group. The overall packing arrangement of **2** closely resembles that of **1**, with TFT and 3tpy molecules arranged in a segregated manner. However, unlike **1**, compound **2** contains only a single set of molecular pairs with aligned olefin groups separated by 3.76 Å.

Single-crystal X-ray diffraction (SXRD) measurements of **2** after ambient light exposure revealed a 50% photoreaction, yielding the intermediate structure $[(TFT)_2(H\text{-}3tpy)_2(H_2\text{-}3ptcb)]$ (**i_{50}2**) (3ptcb = *regio-cis, trans, trans*-1,3-bis(4'-pyridyl)-2,4-bis(3-thiophenyl)cyclobutane). Despite structural differences between **1** and **2**, **i_{50}2** closely resembles **i_{50}1** (Figure S14 and S15). Structural analysis indicated that only alternate olefin pairs underwent reaction, while the separation distance of unreacted pairs increased from 3.76 Å to 3.94 Å (Figure S16). This photoreaction is accompanied by molecular rearrangements, leading to a symmetry similar to **i_{50}1**, with two distinct types of TFT molecules. Time-dimerization studies further confirmed

that **2** undergoes a stepwise photoreaction under ambient light, whereas UV light induces a single-step photoreaction, as demonstrated by a first-order rate constant of 2.06 x 10^{-2} min^{-1}.[47]

Compounds $[(TFT)_2(H\text{-}4spy)_4]$ (**3**) and $[(TFT)_2(H\text{-}3F\text{-}4spy)_4]$ (**4**), where 4spy = 4-styrylpyridine and 3F-4spy = 3'-fluoro-4-styrylpyridine, were synthesized by replacing thiophene with 4spy and 3F-4spy, respectively – both being phenyl- and fluoro-substituted derivatives of 4-vinylpyridine. These molecular systems were designed based on the thiophene-benzene exchange rule, which suggests that thiophene and phenyl rings exhibit similar packing behavior.[48] As anticipated, **3** and **4** displayed packing arrangements closely resembling that of **1** and underwent a stepwise photoreaction, as confirmed by ^{1}H NMR spectroscopy. Although all four compounds exhibited stepwise photoreaction under ambient light, none showed this behavior under UV irradiation, likely due to the rapid reaction kinetics relatively (Table S3). The rate constants, assuming first-order kinetics, were determined as 2.90 x 10^{-2} min^{-1}, 3.24 x 10^{-2} min^{-1} for the compound **3** and **4** respectively (see Figure S40 and S41).[47]

SCSC studies captured key intermediate structures, including $\mathbf{i_{11}3}$ (22% reaction at one site, corresponding to 11% overall conversion) and $\mathbf{i_{72.5}3}$ (100% reaction at one site and 45% at the other, resulting in a 72.5% overall conversion). However, similar to **1**, complete quantitative photoreaction led to crystal degradation, preventing further structural characterization. In the case of **4**, efforts to capture photo products through SCSC studies were also unsuccessful.

Interestingly, crystals of **1**, **2**, and **4** displayed notable mechanical motion upon UV irradiation. After a latency period of 5-6 seconds **1** exhibited a jumping motion along with rotation of the crystals (Figure 2 and the videos in SI), attributed to the strain generated within the unit cell during [2+2] cycloaddition reaction. This might be due to the rapid anisotropic volume expansion in **1** under UV light during the photoreaction.[8] The observed expansion is 0.41%, 0.15%, and 0.24% along the unit cell *a*-, *b*-, and *c*-axes, respectively, with an overall 0.32% unit cell volume increase in the photoproduct $\mathbf{i_{50}1}$ as compared to **1**. Like **1**, compound

2 displayed jumping and flipping motion after 5 seconds of UV light exposure and along with that the luminescence color of the crystal changes from green to blue. In the case of crystal **4**, a portion of the crystal breaks and jumps away from the field of view with very high kinetic energy. This photosalient effect exemplifies the direct conversion of light energy into mechanical energy via a chemical reaction but the photosalient behavior was absent when the crystals are irradiated under sunlight.

To further assess the isostructural nature of the four compounds, a combination of three computational tools – CrystalCMP[49], COMPACK[50], and XPac[51-52] were employed. The analysis revealed one distinct 3D isostructural group comprising **1**, **3**, and **4**, while **2** was identified as an outlier. This distinction in structural symmetry aligns with the earlier observations of packing differences. For added rigor, a second run of XPac analysis was conducted using only **1**, **3**, and **4** with a lower tolerance threshold, which further confirmed their isostructural grouping. The consistency between the results of CrystalCMP, COMPACK, and XPac enhances the reliability of these findings. The isostructural analysis conclusively demonstrates that **1**, **3**, and **4** share isostructural characteristics, whereas **2** deviates due to its distinct structural symmetry (see SI for further details).

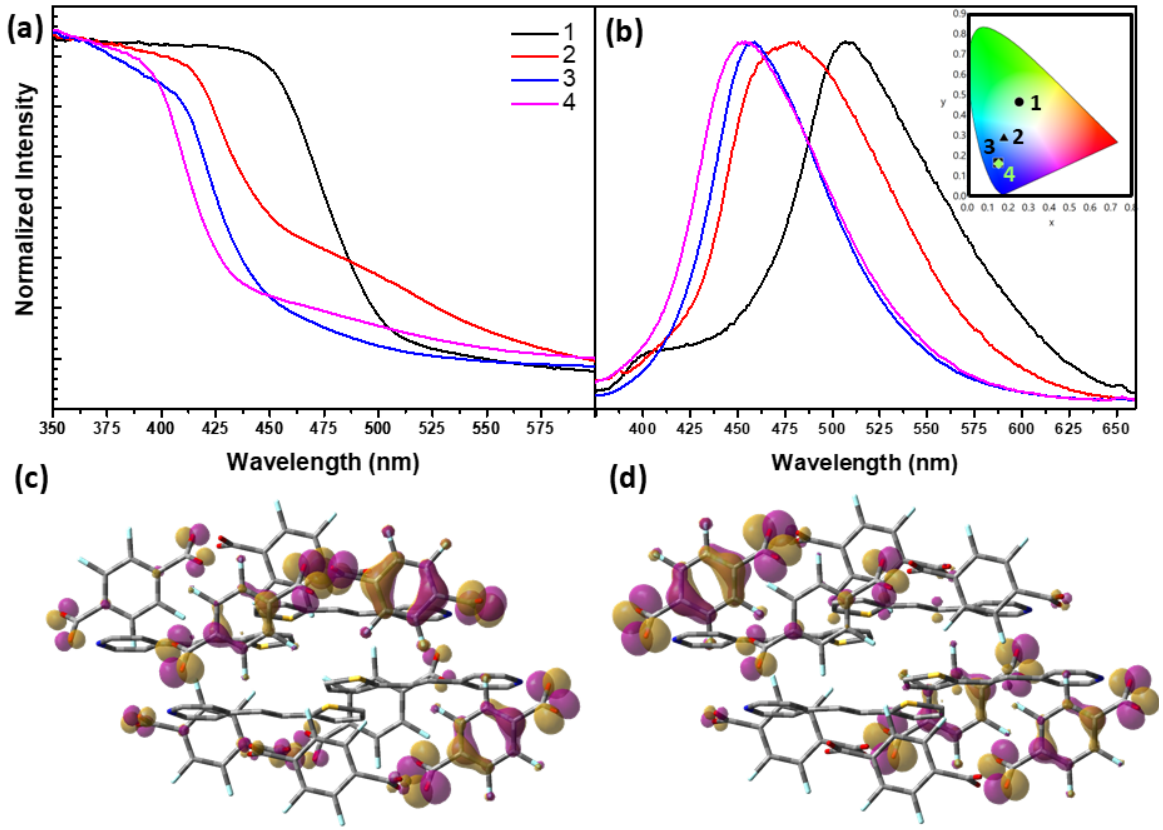

Figure 3. (a) UV-Vis absorption, (b) photoluminescence (inset: CIE coordinates) spectra of **1**, **2**, **3** and **4**. (c) HOMO and (d) LUMO localization of **1** as resulted from TD-DFT calculations.

The optical properties of these compounds were investigated using UV-Vis absorption spectroscopy and photoluminescence (PL) studies. Donor-acceptor (D-A) systems are known for their unique optical behavior due to the formation of new charge-transfer levels absent in the parent molecules.[53] UV-Vis absorption studies revealed that compound **1** exhibits absorption at the highest wavelength, which progressively shifts to lower wavelengths from **2** to **4**, indicating a systematic change in electronic interactions. This trend is further corroborated by simulated absorption spectra (Figure S82 in SI), which show a blue shift from 515 nm to 430 nm moving from **1** to **4**, suggesting enhanced charge transfer or molecular interactions in **2**–**4** compared to **1**. In conjunction with these findings, we have performed TD-DFT

calculations to unfold the localization of (un)occupied molecular orbitals and intermolecular charge transfer. HOMO-3, HOMO-2, HOMO-1, HOMO, LUMO, LUMO+1, LUMO+2, and LUMO+3 orbitals, (Figure 3c, 3d, and S88) are usually involved in optical transitions and we find that there is a transfer of electron density between different HOMOs and LUMOs indicating a through-space charge-transfer in the compounds. i.e., between the TFT and vinylpyridines which are not connected to each other through any chemical bond. See Figures S83 to S87 for the details on the contribution of various atomic orbitals to the HOMO and LUMO for all compounds.

PL studies further supported this trend, with emission peaks shifting from 515 nm (**1**) to 430 nm (**4**). Specifically, compounds **1**, **2**, **3**, and **4** exhibit emissions at 507, 482, 459, and 454 nm, respectively (λ_{ex} = 340 nm) (Figure 3). This progressive blue shift is attributed to the systematic modification of electron density in the 4-vinylpyridine derivatives. The introduction of fluorine in 3F-4spy (compound **4**) leads to the shortest emission wavelength (454 nm) due to its strong electron-withdrawing nature, while 4spy (compound **3**) exhibits a slight red-shift to 459 nm. When the phenyl ring of 4spy is replaced by electron-rich thiophene at the third position (3tpy, compound **2**), the emission shifts further to 482 nm, and thiophene substitution at the second position (2tpy, compound **1**) results in the maximum red-shift at 507 nm. This systematic tuning of optical properties highlights the influence of electron density modulation on emission behavior.

This study successfully demonstrates the tunability of emission wavelengths in isostructural D-A complexes by strategically modifying substituents and their positions, without significantly altering the solid-state structure. To further explore green synthetic approaches, attempts were made to synthesize these D-A systems using solvent-assisted mechanical grinding, minimizing solvent usage. For this, TFT and L (L = 2tpy, 3tpy, 4spy, and 3F-4spy) in a 1:2 molar ratio were ground with 100 µL of DMF for 20 minutes using a mortar and pestle.

The resulting solids were analyzed using powder X-ray diffraction (PXRD), which confirmed the formation of phase-pure compounds **1**–**4** (Figures S10–S13), highlighting the feasibility of a sustainable, solvent-minimized synthesis approach.

Vibrational spectroscopy serves as a valuable tool for assessing changes in the molecular vibrational spectrum due to electron cloud (re)distribution. In this context, we employ Raman spectroscopy to probe the same. In addition, the electronic interaction between the molecules, in general, can also be probed by monitoring the shift of vibrational bands with respect to their isolated counterparts. Figure 4 shows Raman spectrum of **1** compared with its constituents. **1*** indicates the TD-DFT simulated Raman spectrum within 600 to 1460 cm^{-1}. Table S7 shows the spectral position of the Raman peaks and their assignment within 300 to 1750 cm^{-1}. Detailed discussion is given in the SI, while the crucial findings are discussed in the following. It is observed that TFT and 2tpy binds in two configurations (**T1** and **T2**) as shown in Figure 1a and 1b. In correlation with this, some of the modes corresponding to TFT and 2tpy depicted double peaks in **1** and **1*** as identified as **T1** and **T2** on Figure 4. Specifically, the **ν4** of TFT and **ν8**, **ν9** and **ν10** of 2tpy depicted the double peaks. The double peaks are corroborated by the vibrational modes identified in theoretical calculations, where **T1** occurred at lower frequency than that of **T2** except **ν6**. The exception is attributed to the fact that the interaction between TFT and 2tpy is relatively stronger in **T1** that of **T2**, where **ν6*** corresponds to the ring breathing mode. Furthermore, a significant red shift (~12 cm^{-1}) of **ν8** is observed in **1** due to the charge transfer from 2tpy to TFT. A more complex and a series of vibrational modes (**ν12**- **ν18**) are identified corresponding to ring stretching and CH bending modes in 2tpy. These vibrational modes remained in **1**. We note that some of the bands were absent and/or appeared at different frequencies, however identification of specific modes and their assignment was not performed due to the complex interplay of various modes observed in **1***. To summarize, the

splitting and shift of the aforementioned modes of TFT and 2tpy provide us with clear evidence of charge transfer and spectral identification of **T1** and **T2** configurations.

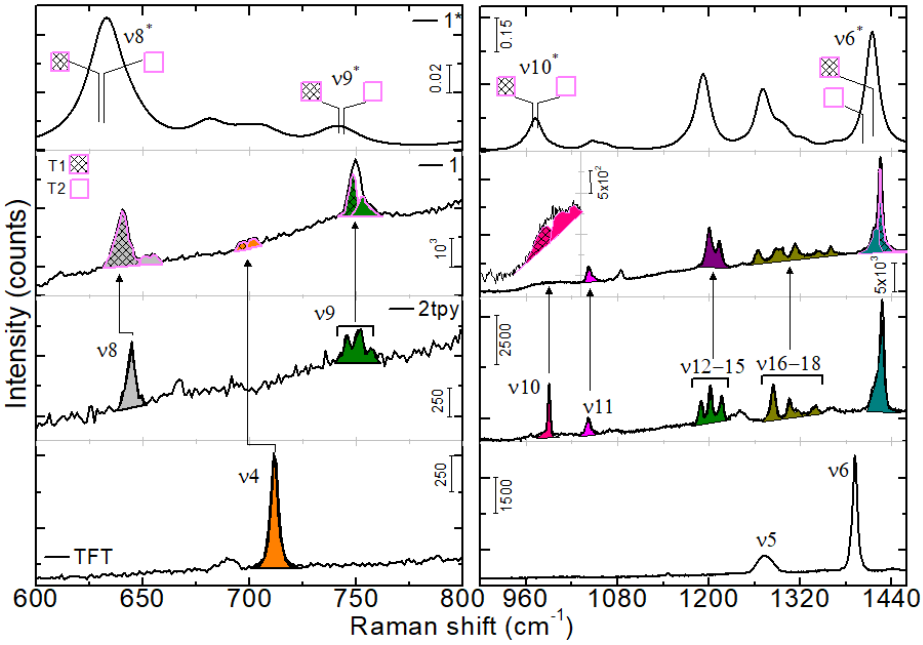

Figure 4. Raman spectra of **1** compared with its constituents within 600 – 800 and 900 – 1460 cm^{-1}. The peak correspondence is color coded across TFT, 2tpy and **1**. Pattern filled (unfilled) correspond to **T1**(2), indicating the 2typ interaction with Type-1(2) TFT while the color provides the correspondence across TFT, 2tpy and **1**. **1*** indicates the computed Raman spectrum, where the units for the intensity scale are $Å^4$/atomic mass units. The peak responses are enumerated.

In summary, four donor–acceptor molecular complexes comprising tetrafluoroterephthalate and 4-vinylpyridine derivatives were synthesized and shown to undergo [2+2] cycloaddition reactions, confirmed by SCSC X-ray diffraction and NMR spectroscopy. All complexes exhibited stepwise photoreactions under ambient light, driven by specific molecular arrangements and charge-transfer interactions, while UV irradiation induced single-step reactions accompanied by distinct photosalient effects. Optical absorption and luminescence studies demonstrated tunable charge-transfer properties without disrupting crystal packing.

Raman spectroscopy, supported by TD-DFT calculations, provided deeper insights into the electronic and vibrational structures of the assemblies. Additionally, a solvent-assisted mechanical grinding approach enabled sustainable synthesis of phase-pure materials. These results establish a versatile platform for developing next-generation photoresponsive crystalline systems, with future work aimed at further tuning electronic and mechanical functionalities through chemical modifications.

ASSOCIATED CONTENT

The supporting information is available free of charge at

Materials and Methods, Synthesis, Powder X-ray Diffraction analysis, X-ray Diffraction Crystallographic data, Structural Analysis of **1**, **2**, **3**, **4**. Time dependent ^{1}H-NMR studies, UV-data, Band gap calculation, Hirshfield Surface Analysis, Thermal analysis, Optical crystal images, Isostructural Analysis, Raman Analysis, Computational Studies (PDF)

Crystal structure of **1** (CIF)

Crystal structure of **2** (CIF)

Crystal structure of **3** (CIF)

Crystal structure of **4** (CIF)

Crystal structure of $\mathbf{i_{50}1}$ (CIF)

Crystal structure of $\mathbf{i_{50}2}$ (CIF)

Crystal structure of $\mathbf{i_{11}3}$ (CIF)

Crystal structure of **i**$_{72.5}$**3** (CIF)

Mechanical motion of **1** Video S1 (mp4)

Mechanical motion of **1** Video S2 (mp4)

Mechanical motion of **2** Video S3 (mp4)

Mechanical motion of **2** Video S4 (mp4)

Mechanical motion of **4** Video S5 (mp4)

Mechanical motion of **4** Video S6 (mp4)

AUTHOR INFORMATION

Corresponding Authors

Dr. R. Medishetty - Department of Chemistry and Department of Materials Science and Metallurgical Engineering, Indian Institute of Technology Bhilai; Orcid ID: 0000-0003-2289-2655. Email: raghavender@iitbhilai.ac.in

Dr. S. Vempati - Department of Physics, IIT Bhilai, Durg, Chhattisgarh 491001, India. Orcid ID: 0000-0002-0536-7827. Email: sesha@iitbhilai.ac.in

Dr. M. M Alam - Department of Chemistry and Department of Materials Science and Metallurgical Engineering, Indian Institute of Technology Bhilai; Orcid ID: 0000-0002-6198-3077

Email: mehboob@iitbhilai.ac.in

Authors

A. Choudhury - Department of Chemistry, Indian Institute of Technology Bhilai, Durg, Chhattisgarh 491002, India; Orcid ID: 0009-0007-4171-6928.

N. Prasad - Department of Physics, Indian Institute of Technology Bhilai, Durg, Chhattisgarh 491002, India. Orcid ID: 0009-0009-6546-4002.

T. Banana - Department of Chemistry, Indian Institute of Technology Bhilai, Durg, Chhattisgarh 491002, India. Orcid ID: 0009-0008-5407-3324.

P. S. Lal - Department of Chemistry, Indian Institute of Technology Bhilai, Durg, Chhattisgarh 491002, India.

Dr. D. S. Hughes - School of Chemistry, Faculty of Engineering and Physical Sciences, University of Southampton, Southampton SO17 1BJ, U.K. Orcid ID: 0000-0001-7032-1676

Dr. N. R. Halcovitch - Chemistry Department, Lancaster University, Faraday Building, Lancaster University, Lancaster, LA1 4YB, UK. Orcid ID: 0000-0001-6831-9681.

Author Contributions

The manuscript was written through contributions of all authors. All authors have given approval to the final version of the manuscript.

# These authors contributed equally.

Funding Sources

AC would like to thank MoE for PMRF PhD fellowship. NP would like to thank MoE and CSIR (09/1237(16807)/2023-EMR-I) for PhD fellowship. SV would like to acknowledge the Science and Engineering Research Board (file no. SRG/2019/001462/PMS) and UGC-DAE CSR (project number CRS/2022-23/01/664), Govt. of India. R.M. acknowledges R. M.

thanks SERB (file no.: SRG/2019/001508) and IBITF (Grant No. IBITF/PRAYAS/Note/2023-24/0009).

Notes

The authors declare no competing financial interest.

ACKNOWLEDGMENT

We thank Dr Veera Reddy, IISER Trivandrum for his continuous support.

REFERENCES

1. Padian, K., Evolution: Doing the locomotion. *Nature* **2016,** *530* (7591), 416-417.

2. Xu, J.; Li, Y.; Yao, Y.; Ding, Y.; Tan, Y.; Hu, G.; Zhang, S.; Zeng, L., A Stimulus-Responsive Optoelectronic Skin From Photonic Crystal. *Adv. Opt. Mater.* **2025**, 2500094.

3. Xie, T., Tunable polymer multi-shape memory effect. *Nature* **2010,** *464* (7286), 267-270.

4. Uchida, E.; Azumi, R.; Norikane, Y., Light-induced crawling of crystals on a glass surface. *Nat. Commun.* **2015,** *6* (1), 7310.

5. Javaid, M.; Haleem, A.; Rab, S.; Pratap Singh, R.; Suman, R., Sensors for daily life: A review. *Sens. Int.* **2021,** *2*, 100121.

6. Zhou, B.; Yan, D., Recent advances of dynamic molecular crystals with light-triggered macro-movements. *Appl. Phys. Rev.* **2021,** *8* (4), 041310.

7. Abendroth, J. M.; Bushuyev, O. S.; Weiss, P. S.; Barrett, C. J., Controlling Motion at the Nanoscale: Rise of the Molecular Machines. *ACS Nano* **2015,** *9* (8), 7746-7768.

8. Awad, W. M.; Davies, D. W.; Kitagawa, D.; Mahmoud Halabi, J.; Al-Handawi, M. B.; Tahir, I.; Tong, F.; Campillo-Alvarado, G.; Shtukenberg, A. G.; Alkhidir, T.; Hagiwara, Y.; Almehairbi, M.; Lan, L.; Hasebe, S.; Karothu, D. P.; Mohamed, S.; Koshima, H.;

Kobatake, S.; Diao, Y.; Chandrasekar, R.; Zhang, H.; Sun, C. C.; Bardeen, C.; Al-Kaysi, R. O.; Kahr, B.; Naumov, P., Mechanical properties and peculiarities of molecular crystals. *Chem. Soc. Rev.* **2023,** *52* (9), 3098-3169.

9. Halabi, J. M.; Ahmed, E.; Catalano, L.; Karothu, D. P.; Rezgui, R.; Naumov, P., Spatial Photocontrol of the Optical Output from an Organic Crystal Waveguide. *J. Am. Chem. Soc.* **2019,** *141* (38), 14966-14970.

10. Irie, M.; Fukaminato, T.; Matsuda, K.; Kobatake, S., Photochromism of Diarylethene Molecules and Crystals: Memories, Switches, and Actuators. *Chem. Rev.* **2014,** *114* (24), 12174-12277.

11. Li, W.; Gately, T. J.; Kitagawa, D.; Al-Kaysi, R. O.; Bardeen, C. J., Photochemical Reaction Front Propagation and Control in Molecular Crystals. *J. Am. Chem. Soc.* **2024,** *146* (47), 32757-32765.

12. Morimoto, K.; Kitagawa, D.; Tong, F.; Chalek, K.; Mueller, L. J.; Bardeen, C. J.; Kobatake, S., Correlating Reaction Dynamics and Size Change during the Photomechanical Transformation of 9-Methylanthracene Single Crystals. *Angew. Chem. Int. Ed.* **2022,** *61* (2), e202114089.

13. Tahir, I.; Ahmed, E.; Karothu, D. P.; Fsehaye, F.; Mahmoud Halabi, J.; Naumov, P., Photomechanical Crystals as Light-Activated Organic Soft Microrobots. *J. Am. Chem. Soc.* **2024,** *146* (44), 30174-30182.

14. Xu, W.; Sanchez, D. M.; Raucci, U.; Zhou, H.; Dong, X.; Hu, M.; Bardeen, C. J.; Martinez, T. J.; Hayward, R. C., Photo-actuators via epitaxial growth of microcrystal arrays in polymer membranes. *Nat. Mater.* **2023,** *22* (9), 1152-1159.

15. Zhu, X.; Xie, M.; Gao, L.; Li, L.; Naumov, P.; Yu, Q.; Wang, G., Combining Simple Deformations to Elicit Complex Motions and Directed Swimming of Smart Organic Crystals with Controllable Thickness. *Angew. Chem. Int. Ed.* **2025,** *64* (5), e202416950.

16. Bhandary, S.; Beliš, M.; Kaczmarek, A. M.; Van Hecke, K., Photomechanical Motions in Organoboron-Based Phosphorescent Molecular Crystals Driven by a Crystal-State [2 + 2] Cycloaddition Reaction. *J. Am. Chem. Soc.* **2022,** *144* (48), 22051-22058.

17. Li, S.; Lu, B.; Fang, X.; Yan, D., Manipulating Light-Induced Dynamic Macro-Movement and Static Photonic Properties within 1D Isostructural Hydrogen-Bonded Molecular Cocrystals. *Angew. Chem. Int. Ed.* **2020,** *59* (50), 22623-22630.

18. Li, S.; Yan, D., Tuning Light-Driven Motion and Bending in Macroscale-Flexible Molecular Crystals Based on a Cocrystal Approach. *ACS Appl. Mater. Interfaces* **2018,** *10* (26), 22703-22710.

19. Mandal, R.; Garai, A.; Peli, S.; Datta, P. K.; Biradha, K., Photoinduced Bending of Single Crystals of a Linear Bis-Olefin via Water-Templated Solid-State [2+2] Photopolymerization Reaction. *Chem. Eur. J.* **2020,** *26* (2), 396-400.

20. Medishetty, R.; Husain, A.; Bai, Z.; Runčevski, T.; Dinnebier, R. E.; Naumov, P.; Vittal, J. J., Single Crystals Popping Under UV Light: A Photosalient Effect Triggered by a [2+2] Cycloaddition Reaction. *Angew. Chem. Int. Ed.* **2014,** *53* (23), 5907-5911.

21. Naumov, P.; Karothu, D. P.; Ahmed, E.; Catalano, L.; Commins, P.; Mahmoud Halabi, J.; Al-Handawi, M. B.; Li, L., The Rise of the Dynamic Crystals. *J. Am. Chem. Soc.* **2020,** *142* (31), 13256-13272.

22. Shi, Y.-X.; Zhang, W.-H.; Abrahams, B. F.; Braunstein, P.; Lang, J.-P., Fabrication of Photoactuators: Macroscopic Photomechanical Responses of Metal–Organic Frameworks to Irradiation by UV Light. *Angew. Chem. Int. Ed.* **2019,** *58* (28), 9453-9458.

23. Biradha, K.; Santra, R., Crystal engineering of topochemical solid state reactions. *Chem. Soc. Rev.* **2013,** *42* (3), 950-967.

24. Liu, Q.; Braunstein, P.; Lang, J.-P., Photoresponsive Coordination Polymer Single Crystal Platforms: Design and Applications. *Acc. Mater. Res.* **2025,** *6* (2), 183-194.

25. Medishetty, R.; Bai, Z.; Yang, H.; Wong, M. W.; Vittal, J. J., Influence of Fluorine Substitution on the Unusual Solid-State [2 + 2] Photo-Cycloaddition Reaction between an Olefin and an Aromatic Ring. *Cryst. Growth. Des.* **2015,** *15* (8), 4055-4061.

26. Nakagawa, M.; Kusaka, S.; Kiyose, A.; Nakajo, T.; Iguchi, H.; Mizuno, M.; Matsuda, R., Beyond the Conventional Limitation of Photocycloaddition Reaction in the Roomy Nanospace of a Metal–Organic Framework. *J. Am. Chem. Soc.* **2023,** *145* (22), 12059-12065.

27. Rath, B. B.; Vittal, J. J., Photoreactive Crystals Exhibiting [2 + 2] Photocycloaddition Reaction and Dynamic Effects. *Acc. Chem. Res.* **2022,** *55* (10), 1445-1455.

28. Wang, M.-F.; Deng, Y.-H.; Hong, Y.-X.; Gu, J.-H.; Cao, Y.-Y.; Liu, Q.; Braunstein, P.; Lang, J.-P., In situ observation of a stepwise [2 + 2] photocycloaddition process using fluorescence spectroscopy. *Nat. Commun.* **2023,** *14* (1), 7766.

29. Akhtaruzzaman; Khan, S.; Dutta, B.; Kannan, T. S.; Kumar Kole, G.; Hedayetullah Mir, M., Cocrystals for photochemical solid-state reactions: An account on crystal engineering perspective. *Coord. Chem. Rev.* **2023,** *483*, 215095.

30. Guo, Q.-H.; Jia, M.; Liu, Z.; Qiu, Y.; Chen, H.; Shen, D.; Zhang, X.; Tu, Q.; Ryder, M. R.; Chen, H.; Li, P.; Xu, Y.; Li, P.; Chen, Z.; Shekhawat, G. S.; Dravid, V. P.; Snurr, R. Q.; Philp, D.; Sue, A. C. H.; Farha, O. K.; Rolandi, M.; Stoddart, J. F., Single-Crystal Polycationic Polymers Obtained by Single-Crystal-to-Single-Crystal Photopolymerization. *J. Am. Chem. Soc.* **2020,** *142* (13), 6180-6187.

31. Juneja, N.; George Iii, G. C.; Hutchins, K. M., Simultaneous Cycloadditions in the Solid State via Supramolecular Assembly. *Angew. Chem. Int. Ed.* **2025,** *64* (3), e202415567.

32. Hutchins, K. M.; Rupasinghe, T. P.; Ditzler, L. R.; Swenson, D. C.; Sander, J. R. G.; Baltrusaitis, J.; Tivanski, A. V.; MacGillivray, L. R., Nanocrystals of a Metal–Organic Complex Exhibit Remarkably High Conductivity that Increases in a Single-Crystal-to-Single-Crystal Transformation. *J. Am. Chem. Soc.* **2014,** *136* (19), 6778–6781.

33. MacGillivray, L. R.; Papaefstathiou, G. S.; Friščić, T.; Hamilton, T. D.; Bučar, D.-K.; Chu, Q.; Varshney, D. B.; Georgiev, I. G., Supramolecular Control of Reactivity in the Solid State: From Templates to Ladderanes to Metal−Organic Frameworks. *Acc. Chem. Res.* **2008,** *41* (2), 280-291.

34. Li, C.; MacGillivray, L. R., Supramolecular Matter Through Crystal Engineering: Covalent Bond Formation to Postsynthetic Modification. *Chem. Eur. J.* **2025,** *31* (27), e202500756.

35. Khan, S.; Dutta, B.; Mir, M. H., Impact of solid-state photochemical [2+2] cycloaddition on coordination polymers for diverse applications. *Dalton Trans.* **2020,** *49* (28), 9556-9563.

36. Kole, G. K.; Mir, M. H., Isolation of elusive cyclobutane ligands via a template-assisted photochemical [2 + 2] cycloaddition reaction and their utility in engineering crystalline solids. *CrystEngComm.* **2022,** *24*, 3993-4007.

37. Wang, M.-F.; Mi, Y.; Hu, F.-L.; Hirao, H.; Niu, Z.; Braunstein, P.; Lang, J.-P., Controllable multiple-step configuration transformations in a thermal/photoinduced reaction. *Nat. Commun.* **2022,** *13* (1), 2847.

38. Ferraris, J.; Cowan, D. O.; Walatka, V.; Perlstein, J. H., Electron transfer in a new highly conducting donor-acceptor complex. *J. Am. Chem. Soc.* **1973,** *95* (3), 948-949.

39. Goetz, K. P.; Vermeulen, D.; Payne, M. E.; Kloc, C.; McNeil, L. E.; Jurchescu, O. D., Charge-transfer complexes: new perspectives on an old class of compounds. *J. Mater. Chem. C,* **2014,** *2* (17), 3065-3076.

40. Barman, D.; Annadhasan, M.; Bidkar, A. P.; Rajamalli, P.; Barman, D.; Ghosh, S. S.; Chandrasekar, R.; Iyer, P. K., Highly efficient color-tunable organic co-crystals unveiling polymorphism, isomerism, delayed fluorescence for optical waveguides and cell-imaging. *Nat. Commun.* **2023,** *14* (1), 6648.

41. Gracin, D.; Štrukil, V.; Friščić, T.; Halasz, I.; Užarević, K., Laboratory Real-Time and In Situ Monitoring of Mechanochemical Milling Reactions by Raman Spectroscopy. *Angew. Chem. Int. Ed.* **2014,** *53* (24), 6193-6197.

42. Julien, P. A.; Arhangelskis, M.; Germann, L. S.; Etter, M.; Dinnebier, R. E.; Morris, A. J.; Friščić, T., Illuminating milling mechanochemistry by tandem real-time fluorescence emission and Raman spectroscopy monitoring. *Chem. Sci.* **2023,** *14* (43), 12121-12132.

43. Lien Nguyen, K.; Friščić, T.; Day, G. M.; Gladden, L. F.; Jones, W., Terahertz time-domain spectroscopy and the quantitative monitoring of mechanochemical cocrystal formation. *Nat. Mater.* **2007,** *6* (3), 206-209.

44. Lukin, S.; Užarević, K.; Halasz, I., Raman spectroscopy for real-time and in situ monitoring of mechanochemical milling reactions. *Nature Protocols* **2021,** *16* (7), 3492-3521.

45. Michalchuk, A. A. L.; Emmerling, F., Time-Resolved In Situ Monitoring of Mechanochemical Reactions. *Angew. Chem. Int. Ed.* **2022,** *61* (21), e202117270.

46. Schmidt, G. M. J., Photodimerization in the solid state. *Pure & Appl. Chem.* **1971,** *27*, 647-678.

47. Please note that the absorbance and surface features also play a role in determining the quantum yield of the reaction (see SI for the details on the photon flux).

48. Thallapally, P. K.; Chakraborty, K.; Carrell, H. L.; Kotha, S.; Desiraju, G. R., Shape and size effects in the crystal structures of complexes of 1,3,5-trinitrobenzene with some trigonal donors: The benzene-thiophene exchange rule. *Tetrahedron* **2000,** *56* (36), 6721-6728.

49. Rohlíček, J.; Skořepová, E.; Babor, M.; Čejka, J., CrystalCMP: an easy-to-use tool for fast comparison of molecular packing. *J. Appl. Crystallogr.* **2016,** *49* (6), 2172-2183.

50. Chisholm, J. A.; Motherwell, S., COMPACK: a program for identifying crystal structure similarity using distances. *J. Appl. Crystallogr.* **2005,** *38* (1), 228-231.

51. Gelbrich, T.; Hursthouse, M. B., A versatile procedure for the identification, description and quantification of structural similarity in molecular crystals. *CrystEngComm.* **2005,** *7* (53), 324-336.

52. Gelbrich, T.; Threlfall, T. L.; Hursthouse, M. B., XPac dissimilarity parameters as quantitative descriptors of isostructurality: the case of fourteen 4,5′ -substituted benzenesulfonamido-2-pyridines obtained by substituent interchange involving CF3/I/Br/Cl/F/Me/H. *CrystEngComm.* **2012,** *14* (17), 5454-5464.

53. Pluczyk-Malek, S.; Honisz, D.; Akkuratov, A.; Troshin, P.; Lapkowski, M., Tuning the electrochemical and optical properties of donor-acceptor D-A2-A1-A2-D derivatives with central benzothiadiazole core by changing the A2 strength. *Electrochim. Acta* **2021,** *368*, 137540.

Table of Contents: